Chapter 5.

A rapid, label-free, and quantitative method for characterizing binding properties of RNA aptamers

Abstract

Aptamers are nucleic acid sequences that are capable of binding molecular ligands with high affinities and provide important functional components for construction of synthetic genetic devices. RNA aptamers are typically generated *de novo* through iterative *in vitro* selection strategies to isolate sequences that bind small molecule ligands with high affinities and specificities from large nucleic acid libraries. Small molecule RNA aptamers have traditionally been characterized through isocratic elution and equilibrium filtration methods. However, these methods require labeling of molecules, thereby limiting their general applicability to characterize many RNA-small molecule pairs. Newer methods based on isothermal titration calorimetry (ITC) offer the potential of providing a label-free aptamer characterization strategy, but the requirement of large quantities of homogenous RNA makes the ITC-based method difficult to scale for the characterization of many RNA-ligand pairs. Here, we describe a rapid, label-free, and flexible aptamer characterization strategy based on surface plasmon resonance (SPR). We utilized a sensor surface modified with a DNA linker to capture the RNA aptamer that contains a complementary sequence to the DNA linker through hybridization. The small molecule ligand in free solution is injected over the RNA-hybridized surface to monitor binding interactions in real time. The rate of SPR signal change is fit to mathematical models to obtain associated thermodynamic and kinetic parameters. We validated the SPR-based method on several previously characterized RNA aptamers. Our SPR-based strategy requires little sample consumption and can be quickly tailored to qualitatively screen or quantitatively characterize many small molecule-RNA pairs.

5.1 Introduction

Aptamers are nucleic acid sequences that are capable of binding molecular ligands with high affinities (1). RNA aptamers are typically generated *de novo* through an iterative *in vitro* selection strategy or SELEX (*S*ystematic *E*volution of *L*igands by *EX*ponential enrichment) (2,3) or obtained from naturally-occurring sequences (4-6). RNA aptamers have been generated through *in vitro* selection strategies to many small molecule ligands, including alkaloids, amino acids, and oligosaccharides (1). By incorporating appropriate counterselection cycles in the selection process, aptamers have been selected *in vitro* to discriminate between structurally similar molecules. In one example, an aptamer selected to theophylline exhibits a 10,000-fold lower affinity for caffeine, which differs from theophylline by a single methyl group (7).

Binding affinities of small molecule RNA aptamers are typically determined by isocratic elution (8,9) or equilibrium filtration (7,9-11). Both methods require labeling of molecules (RNA or small molecule, respectively) and provide a low-throughput process for obtaining binding affinities. More recently, a label-free analytical method, isothermal titration calorimetry (ITC), has been used to characterize small molecule aptamers by measuring heat generation or absorption associated with the binding interactions (5,12). However, the ITC-based method requires large quantities of homogenous RNA, which limits its ability to be applied to the characterization of many RNA-small molecule pairs. In addition, all of these methods are limited to thermodynamic analysis of binding interactions, whereas for many applications information on binding kinetics are also desired.

Progress in biosensor technologies has led to the development of platforms based on surface plasmon resonance (SPR), which allows for the real-time, label-free detection of biomolecular interactions (13). The SPR-based biosensor platform involves immobilization of one molecule (ligand) on a sensor surface and monitoring its interaction with another molecule (analyte) in solution. The association or dissociation of the ligand-analyte complex results in a change in the refractive index, which is associated with the local mass density, near the sensor surface. The refractive index change is converted into an SPR signal, which is expressed in resonance units (RU). The rate of SPR signal change is fit to a mathematical model to acquire thermodynamic and kinetic parameters, including binding affinities, association rates, and disassociation rates. One of the pioneering SPR platforms, Biacore, has been applied to characterize thermodynamic and kinetics properties of diverse biomolecular interactions, including protein-protein (14), nucleic acid-protein (15), small molecule-nucleic acid (16), and small molecule-protein (17,18) interactions. In addition, the Biacore platform utilizes a microfluidic-based flow system that requires small sample volumes, thereby presenting a significant advantage over the ITC-based method.

Small molecule binding interactions have been challenging for the SPR-based methods to characterize due to the small local mass density change (19). The maximum expected SPR binding response is proportional to the ligand immobilization level on the sensor surface, analyte-to-ligand molecular weight ratio, and number of available binding sites on the ligand (20). Researchers have previously chosen to immobilize small molecule ligands on the sensor surface, such that binding of the corresponding RNA analyte resulted in a large binding response due to the large analyte-ligand molecular

weight ratio (16,21-24). However, this strategy requires the small molecule ligands to have or be modified with appropriate functional groups, such as the amine, thiol, maleimide, or aldehyde groups, for the conjugation chemistry to attach the ligand to the sensor surface and is therefore not scalable to the characterization of many diverse RNA-small molecule pairs. In addition, such conjugation strategies may impact functional groups that play a role in the ligand binding interactions and thus impact measured ligand binding properties.

We describe a rapid, quantitative aptamer characterization strategy based on the Biacore biosensor platform. An efficient strategy was developed for capturing RNA aptamers to the sensor surface, by appending a common binding sequence to the 5' end of each RNA aptamer sequence and covalently coupling a DNA linker sequence to the sensor surface, which serves to capture the modified aptamer sequences through programmed hybridization interactions. Small molecule analytes in solution were injected over the sensor surface to monitor binding interactions in real time. An efficient regeneration strategy was developed to remove the captured RNA from the sensor surface upon completion of the assay to allow for characterization of multiple RNA-small molecule pairs on the same sensor surface. We validated the SPR-based aptamer characterization strategy by measuring the binding properties of theophylline, citrulline, and arginine aptamers and compared the measured values to those determined by isocratic elution or equilibrium filtration. Our SPR-based strategy supports the rapid characterization of binding properties for RNA aptamers to small molecule ligands, thereby providing a powerful characterization tool for functional RNA design.

5.2 Results

5.2.1 Development of a SPR-based binding assay to characterize RNA-small molecule binding interaction

We developed a capture-based binding assay by indirectly immobilizing RNA through hybridization to a DNA linker sequence which is covalently coupled to the sensor surface (Figure 5.1). By capturing RNA to the sensor surface, small molecule analytes can be directly diluted in solution and injected over the sensor surface, thereby avoiding limitations associated with conjugating the small molecule to the sensor surface. The sensor surface for the binding assay is generated by covalently coupling a 24-mer poly-T DNA linker with an amino modification on the 5' end to a dextran-based sensor surface through an EDC-mediated amine coupling reaction. Each sensor surface includes two flow cells (FC1 and FC2), and both FCs were modified with the poly-T DNA linker. FC1 is used as a reference flow cell to correct for bulk refractive index changes, matrix effects, nonspecific binding, injection noise and baseline drift (25). The DNA linker allows the capture of RNA containing a 24-mer poly-A tail, which is appended to the 3' end of the RNA sequence to FC2 through hybridization. It is expected that the poly-A sequence interferes minimally with the native aptamer structure.

The DNA linker is coupled at high density (~4000 RU) to the sensor surface to increase the amount of RNA captured and therefore increase the small molecule binding signal. For a typical small molecule (>150 Da) binding assay, the capture of a 30 kDa RNA to ~1500 RU is sufficient to generate a reliable and measurable binding signal (>5 RU). The small molecule analyte at a particular concentration is subsequently injected over the sensor surface, and the SPR signal change associated with the binding

interaction is monitored. Since the capture of the RNA aptamer to the sensor surface is based on hybridization interactions with the DNA linker, a nucleic acid denaturant, such as 25 mM NaOH, can be injected to remove the RNA from the surface, thereby allowing reuse of the sensor surface to measure the binding signal at varying analyte concentrations.

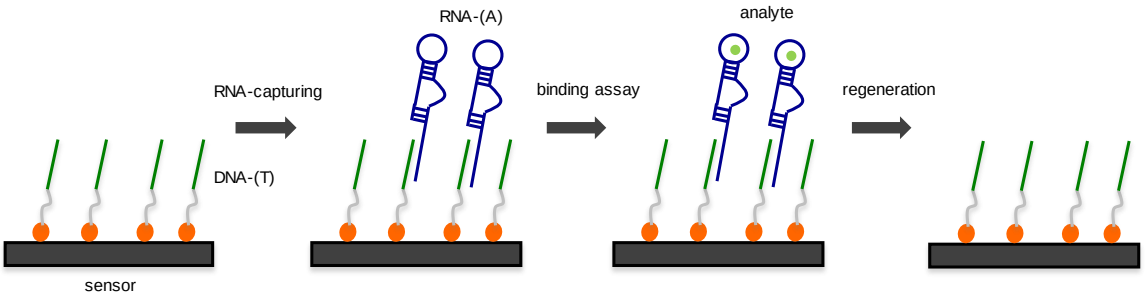

Figure 5.1 Schematic of the SPR-based RNA-small molecule binding assay. The sensor surface is generated by covalently linking a 5' amino-modified poly-T DNA strand to the carboxymethyl dextran sensor surface via an EDC-mediated amine coupling reaction. RNA, with a poly-A sequence at its 3'end, is hybridized to the DNA linker, followed by the injection of small molecule analyte to monitor binding interactions in real time. The surface is regenerated with 25 mM NaOH for the next assay.

5.2.2 Validation of the SPR-based aptamer binding assay

We applied our SPR-based method to measure the binding properties of three aptamer sequences that have been extensively characterized through different methods: the theophylline, citrulline, and arginine aptamers (7,9) (Figure 5.2). The theophylline aptamer has been characterized to have a binding affinity of 0.2-0.4 μM by equilibrium filtration (7) and fluorescence stopped-flow methods (26). The citrulline and arginine aptamers have been characterized by both isocratic elution and equilibration filtration methods to have a binding affinities of 62-68 and 56-76 μM, respectively (9). We performed the SPR-based binding assays on these three aptamer sequences at a series of

concentrations that span ~10-fold above and below the expected binding affinities for proper analysis (Figure 5.3). As proper formation of RNA tertiary structure can be dependent on $MgCl_2$ concentrations, the ligands were directly dissolved in the binding characterization buffer (10 mM HEPES, 150 mM NaCl, 5 mM $MgCl_2$, and 0.05% P20 surfactant, pH7.4) comprising the same $MgCl_2$ concentration as that used in the buffers used in the *in vitro* selection of these aptamers (26). The binding characterization buffer was also used as the Biacore running buffer to equilibrate the instrument.

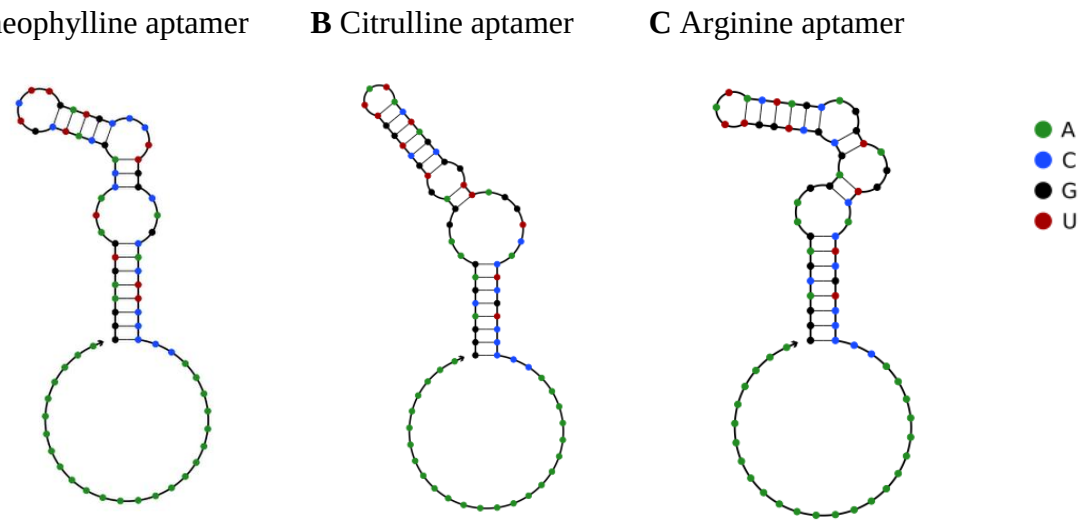

Figure 5.2 Predicted secondary structures of RNA aptamers with a 24-mer poly-A tail appended to the 3' end. The secondary structures of (A) theophylline, (B) citrulline, and (C) arginine aptamers were generated using Nupack by setting the temperature to 25ºC (27). The sequence for each aptamer is provided in Supplementary Table S5.1.

For the characterization of the theophylline aptamer, three independent replicated binding assays were performed. Each binding assay consists of multiple assay cycles, and each cycle includes an RNA-capture, theophylline-injection, and regeneration steps. For each assay cycle, ~10-50 ng/µl of RNA was captured onto the sensor surface for 2 minutes at a flow rate of 2 µl/min, resulting in an ~1700-2000 RU of RNA-capture level.

The RNA-capture levels were highly consistent within each replicate, with a coefficient of variation (CV) less than 0.46%. Varying concentrations of theophylline were injected over the sensor surface in random orders (0.56, 1.67, 0.19, 5, 0.06, and 0 μM) (Figure 5.3A). In between each injection of theophylline, the captured RNA was removed by an injection of 25 mM NaOH for 30 seconds at a flow rate of 30 μl/min, and new RNA was re-captured onto the sensor surface prior to the injection of next theophylline sample.

The sensorgrams from FC2 were referenced first by subtracting the corresponding sensorgrams from FC1 to correct for bulk refractive index changes, matrix effects, nonspecific binding, injection noise and baseline drift (25). The reference-subtracted sensorgram (FC2-FC1) was double-referenced by subtracting the sensorgram associated with the blank injection (0 μM) to account for any systematic drift over the course of the injection (Figure 5.3A). The double-referenced sensorgram was fit to a 1:1 kinetic binding model (Supplementary Figure S5.1) and a steady-state affinity model (Supplementary Figure S5.2). The association ($1.46\times10^{5} \pm 7.32\times10^{3}$ $M^{-1}s^{-1}$) and dissociation ($6.31\times10^{-2} \pm 4.72\times10^{-3}$ s^{-1}) rates were determined for the theophylline aptamer. The binding affinity (433 ± 37.8 nM) obtained from calculating the ratio of the dissociation over association constants was in close agreement with that obtained from the steady-state affinity model (324 ± 22.9 nM).

Similar binding assays and analyses were performed on the citrulline (Supplemental Figure S5.3) and arginine (Supplemental Figure S5.4) aptamers. For the characterization of citrulline and arginine aptamers, the RNA-capture level ranged from ~2200-2300 RU and ~1900-2100 RU, respectively. Varying concentrations of citrulline/arginine were injected over the sensor surface in random orders (0.56, 1.67,

0.19, 5, 0.06, and 0 μM) (Figure 5.3B and C). Kinetic analysis for the citrulline and arginine aptamers was not possible because the fast kinetic rates exceeded the machine detection limit (association rate: 10^3-10^7 $M^{-1}s^{-1}$; dissociation rate: 10^{-5}-0.1 s^{-1}). Binding affinities for the citrulline (23.2 ± 0.21 μM) and arginine (15.9 ± 0.32 μM) aptamers were obtained from the steady-state affinity model. For the arginine aptamer, the assay performed at 500 μM arginine was excluded from the analysis due to non-specific binding to the reference flow cell (Figure 5.3C and Supplementary Figure S5.4). The measured affinities for the three aptamers were in close agreement with those obtained by the more traditional methods, thus validating our SPR-based binding assay.

A Theophylline aptamer

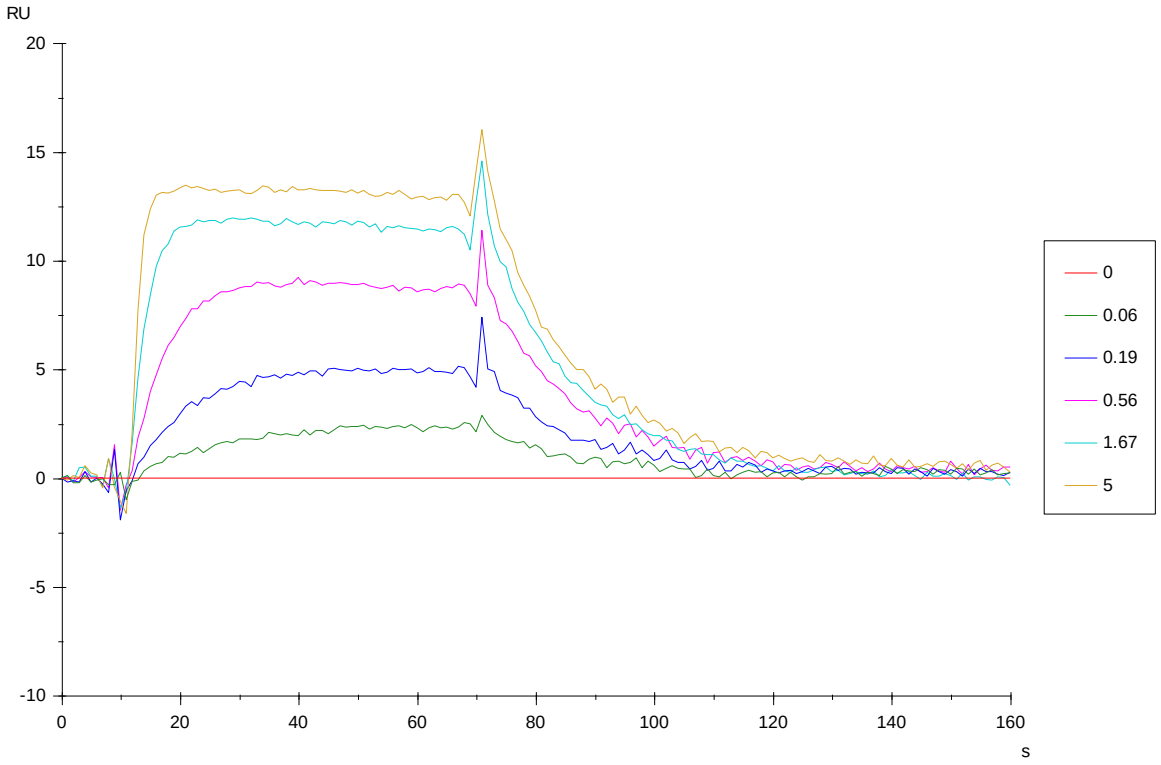

B Citrulline aptamer

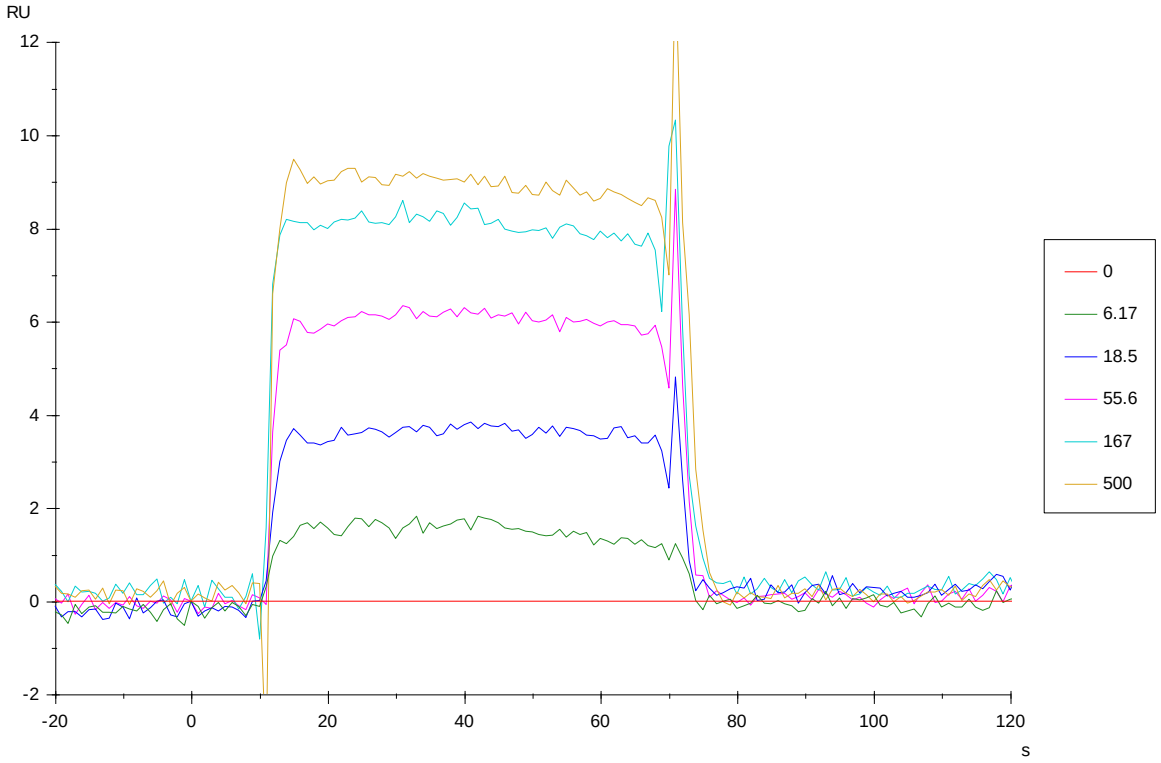

C Arginine aptamer

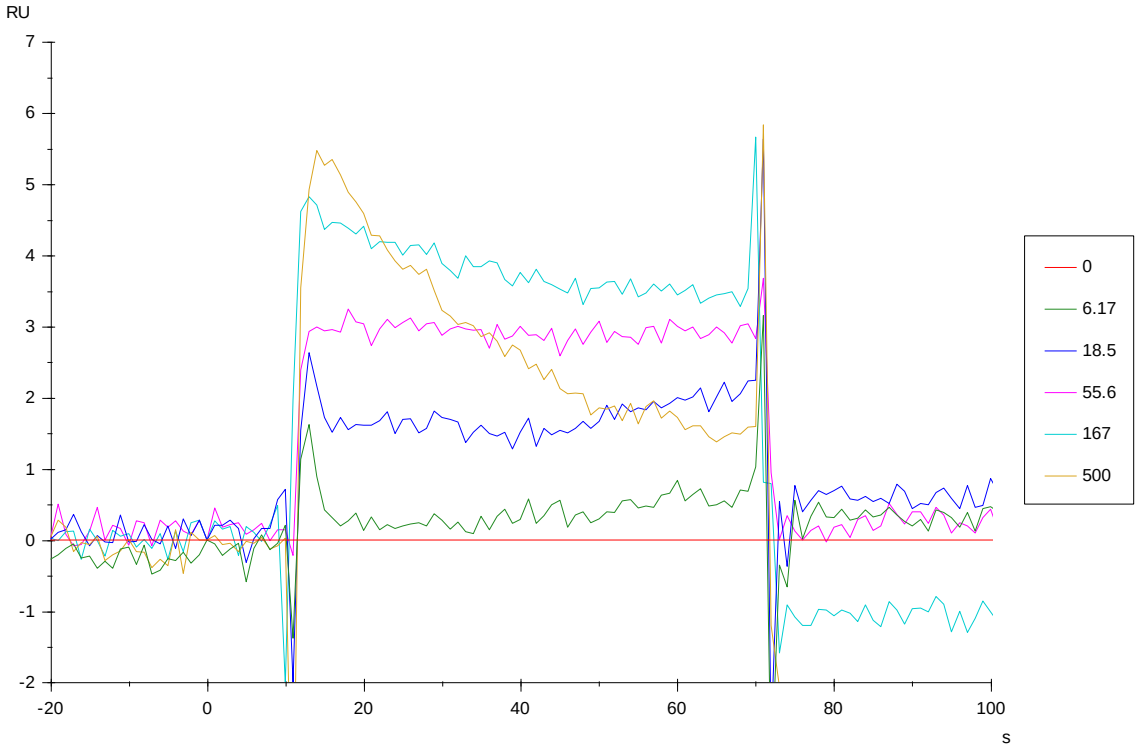

Figure 5.3 Biacore response (RU) as a function of time (s). Representative Biacore sensorgrams for (A) theophylline, (B) citrulline, and (C) arginine aptamers are shown here. The sensorgrams were double-referenced by the reference flow cell (FC1) and the blank injection as described in the main text. The indicated concentrations are in μM.

5.3 Discussion

We developed a rapid, flexible SPR-based aptamer characterization strategy that can be applied for the characterization of many aptamer-small molecule ligand binding interactions. By appending a common hybridization sequence to the RNA aptamer, we can capture different RNA sequences to the same sensor surface, thereby presenting a more cost-effective strategy than direct coupling of the RNA sequence to the sensor surface (23). A similar RNA-capture strategy has been previously employed for the characterization of RNA-protein binding interactions by immobilizing a biotin-modified DNA linker to a streptavidin-based sensor surface (28). Although the streptavidin-biotin binding interaction is essentially irreversible, with a dissociation constant of ~1 fM, the protein-based sensor surface is less resilient to the harsh denaturant (25 mM NaOH) used in our strategy to regenerate the surface. We chose to covalently immobilize the DNA linker to the dextran-based sensor surface, as the dextran is highly resistant to harsh chemicals, thereby increasing the stability of the characterization surface for many binding assays. In addition, for the Biacore system used in our strategy the dextran-based surface offers more reactive sites than the protein-based sensor surface for the immobilization of DNA linker. Therefore, by using a dextran-based sensor surface higher RNA-capture levels can be achieved, allowing a higher small molecule binding signal.

We demonstrated that our method is quantitative and yields similar values for thermodynamic binding properties as those obtained through the more traditional

methods based on equilibrium filtration or isocratic elution. Our SPR-based strategy allows measurements of kinetic parameters in addition to equilibrium parameters and requires little sample volume due to its microfluidic-based flow system, thereby providing a significant advantage over the ITC-based method. One limitation to our assay is in the possibility of non-specific interactions between the small molecule analyte and the sensor surface, particularly at high analyte concentrations. However, the extent of non-specific interactions may be eliminated or reduced by optimizing the characterization buffer.

By developing a flexible and rapid capture-based assay method, our strategy can be readily coupled to *in vitro* aptamer selection strategies to allow for: (i) screening of enriched aptamer libraries for qualitative (yes/no) binding; (ii) ranking of functional aptamer sequences based on their affinities; (iii) identifying consensus sequences through systematic truncation of functional aptamer sequences; and (vi) screening for specificities against a family of molecules that share structural similarities. Furthermore, our strategy can be applied to characterize binding interactions between nucleic acids (DNA, RNA) and diverse molecules (small molecules, DNA, RNA, proteins), or further extended to monitoring binding to more complex RNA molecules, such as synthetic RNA devices (29). Thus, the described SPR-based strategy provides a versatile and powerful tool for advancing functional RNA design.

5.4 Materials and Methods

5.4.1 *In vitro* transcription of RNA aptamers

DNA synthesis was performed by Integrated DNA Technologies (Coralville, IA) or the Protein and Nucleic Acid Facility (Stanford, CA). Aptamers with the poly-A sequence were prepared through a T7 transcription reaction using PCR products amplified from templates using forward and reverse primers Biacore-fwd (5'-TTCTAATACGACTCACTATAGG) and Biacore-rev (5'-TTTTTTTTTTTTTTTTTTTTTTTTTTTGGGG), respectively. All described aptamer template sequences are summarized in Supplementary Table S5.1. A total of 1-2 μg of PCR product was transcribed in a 25 μl reaction, consisting of the following components: 1×RNA Pol Reaction Buffer (New England Biolabs, Ipswich, MA), 2.5 mM of each rNTP, 1 μl RNaseOUT (Invitrogen, Carlsbad, CA), 10 mM $MgCl_2$, and 1 μl T7 Polymerase (New England Biolabs). After incubation at 37°C for 2 hr, NucAway Spin Columns (Ambion, Austin, TX) were used to remove unincorporated nucleotides from the transcription reactions according to the manufacturer's instructions.

5.4.2 Biacore sensor chip surface generation

Biosensor experiments were performed on a Biacore X100 instrument (Biacore, Uppsala, Sweden) at 25ºC. A CM5 sensor chip (Biacore) was docked in the Biacore X100 and equilibrated with the HBS-P buffer (Biacore) (10 mM HEPES, 150 mM NaCl, pH 7.4, 0.05% Surfactant P20) supplemented with 5 mM $MgCl_2$. The DNA linker strand (5'-TTTTTTTTTTTTTTTTTTTTTTTT), with an amino modification on the 5' end, was immobilized to the chip surface via standard amine-coupling chemistry. Briefly, the

carboxymethyl surface of the CM5 chip was activated for 7 min at a flow rate of 5 μl/min using a 1:1 volume ratio of 0.4 M 1-ethyl-3-(3-dimethylaminopropyl) carbodiimide (Biacore) and 0.1 M N-hydroxysuccinimide (Biacore). A molar ratio of 1:60 of DNA strand to cetyl trimethylammonium bromide (Amresco, Solon, OH) was diluted in 10 mM HEPES buffer (Sigma, St. Louis, MO) to a final concentration of 10 μM and 0.6 mM, respectively, and injected over the activated surface for 10 min at a flow rate of 5 μl/min. Excess activated groups were blocked by an injection of 1 M ethanolamine (Biacore), pH 8.5, for 7 min at a flow rate of 5 μl/min. The immobilization reaction was performed sequentially on both flow cells (FC1, FC2), where FC1 was used as a reference cell to correct for bulk refractive index changes, matrix effects, nonspecific binding, injection noise and baseline drift (25). Approximately 3000 RU of the DNA strand was immobilized using this protocol.

5.4.3 SPR-based aptamer binding assays

The Biacore X100 instrument was primed three times with the running buffer (HBS-P + 5 mM $MgCl_2$) prior to all binding assays. For each assay, five startup cycles were performed to stabilize the sensorgram baseline. For each startup cycle, the transcribed aptamer construct (~10-50 ng/μl) was captured onto the reaction flow cell (FC2) for 2 min at a flow rate of 2 μl/min (~1700~2300 RU), followed by an injection of 25 mM NaOH for 30 sec at a flow rate of 30 μl/min over both flow cells to regenerate the sensor surface. Dilution series of the ligand were made up in the running buffer and injected in random orders. Each concentration sample was injected over both flow cells for 60 sec at a flow rate of 30 μl/min, followed by a 90-sec dissociation phase during

which the running buffer flows over the sensor surface. The remaining RNA was removed by an injection of 25 mM NaOH for 30 sec at a flow rate of 30 μl/min over both flow cells, and RNA can be re-captured onto the sensor surface for the next assay cycle.

Data processing and analysis were performed using Biacore X100 Evaluation Software v2.0 (Biacore). A double-referencing method was performed to process all datasets (30). In brief, data from the reaction flow cell (FC2) was referenced first by subtracting data from the reference flow cell (FC1) to correct for bulk response due to differences in sample compositions. The reference-subtracted data (FC2-FC1) was referenced again by a blank injection (running buffer) to account for any systematic drift over the course of the injection. The double-referenced data was fit to the default 1:1 binding model for kinetic analysis (Supplementary Figure S5.2) or steady-state affinity model for thermodynamic analysis (Supplementary Figure S5.3). Reported values are the mean of at least three independent experiments.

5.5 Supplementary Information

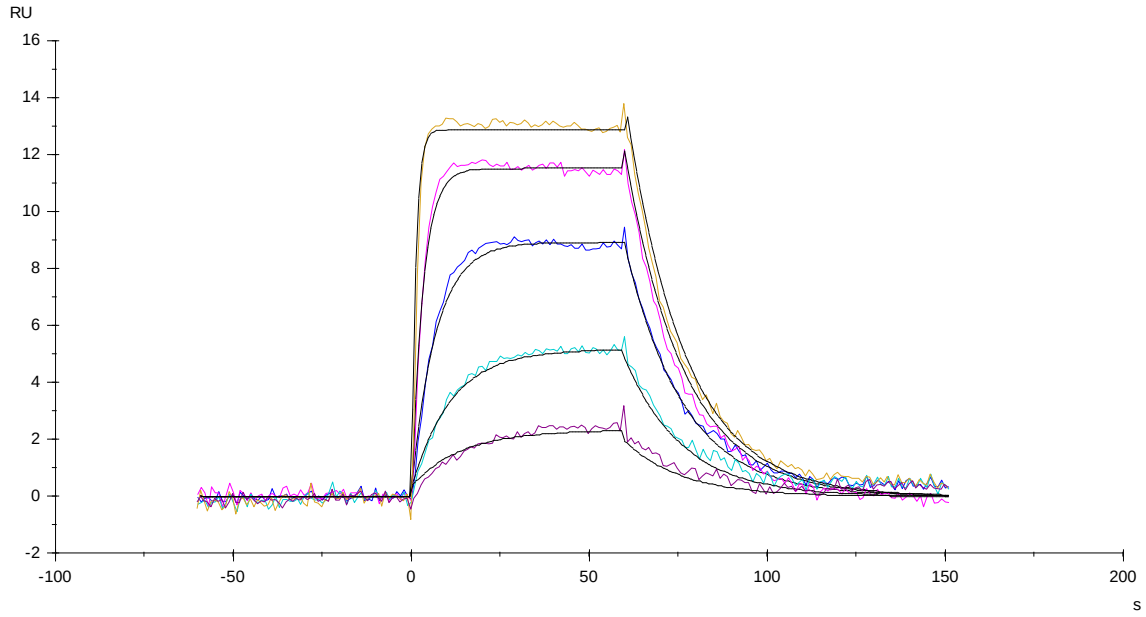

Conc. (µM)	RNA (RU)	ka (1/Ms)	kd (1/s)	KD (M)	RI (RU)
0.56	1994	1.54E+05	0.06077	3.96E-07	0.123
1.67	1993	**Rmax (RU)**	**tc**	**Chi² (RU²)**	-0.6335
0.19	1996	15.05	3.58E+10	0.0938	0.2921
5	1991				-1.048
0.06	1988				0.364
Mean	1992	**CV**	0.14%		

Supplementary Figure S5.1 Biacore 1:1 kinetic binding model for the theophylline aptamer sequence. The double-referenced sensorgrams for theophylline binding assays were fit to a 1:1 kinetic binding model (A+B↔AB): dA/dt = (tc*flow rate^(1/3))*(Conc-A) - (ka*A*B - kd*AB); dB/dt = - (ka*A*B - kd*AB); dAB/dt = (ka*A*B - kd*AB); Total response = AB + RI, with initial values A[0] = 0; B[0] = Rmax (maximum binding signal); AB[0] = 0. A, B, and AB represents the small molecule analyte concentration (Conc), unbound RNA, and small molecule-RNA complex. The model was fit to the sensorgrams to obtained tc (mass transfer constant), ka (association constant), kd (dissociation constant), Rmax, and RI (residuals). One representative fitted replicate is shown here. Small Chi^2 values indicate that the fitted values are close to the observed values.

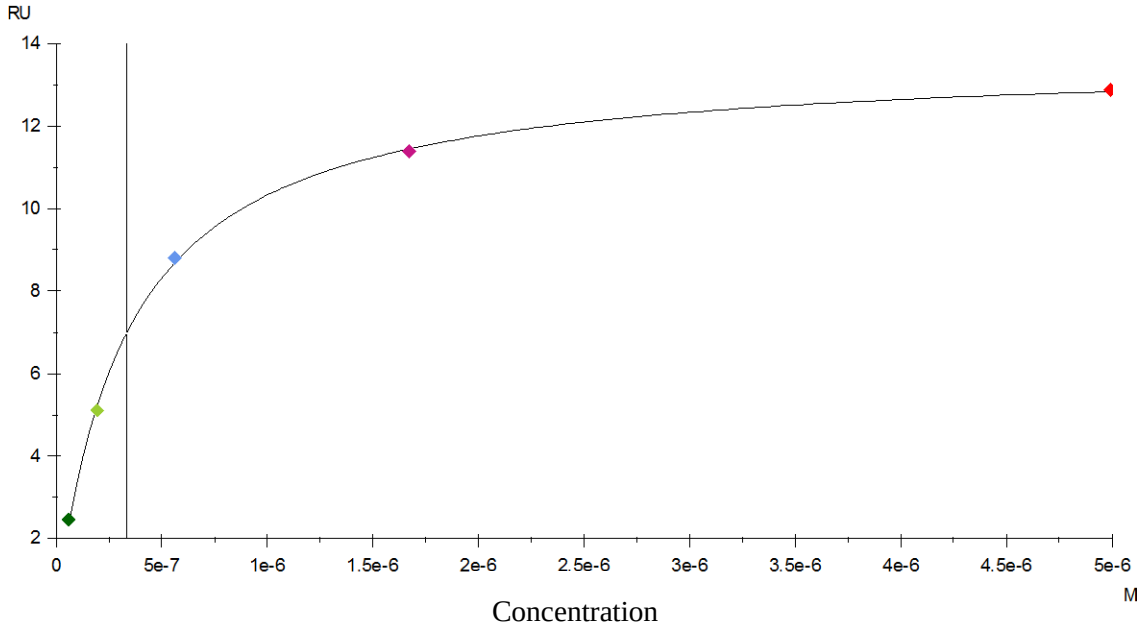

KD (M)	Rmax (RU)	offset (RU)	Chi² (RU²)
3.37E-07	13.29	0.3887	0.0145

Supplementary Figure S5.2 Biacore steady-state affinity model for the theophylline aptamer sequence. The double-referenced sensorgrams for theophylline binding assays were fit to a steady-state affinity model: Conc*Rmax/(Conc+KD)+offset. The model was fit to the sensorgrams to obtained KD (binding affinity), Rmax (maximum binding signal), and offset (residuals). One representative fitted replicate is shown here. The top sensorgram shows the steady state RU taken for the affinity analysis. The bottom sensorgram shows the fitted curve against the experimental values. Small Chi^2 values indicate that the fitted values are close to the observed values.

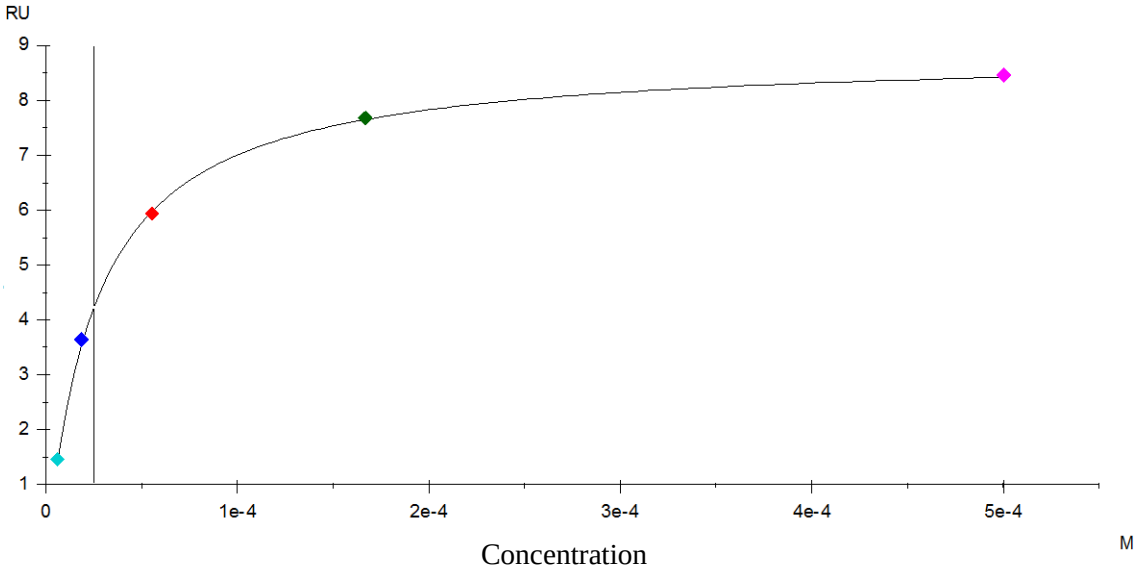

KD (M)	Rmax (RU)	offset (RU)	Chi² (RU²)
2.51E-05	9.242	-0.3783	0.00514

Supplementary Figure S5.3 Biacore steady-state affinity model for the citrulline aptamer sequence. The sensorgrams from the citrulline binding assays were fit to a steady-state affinity model as described in Supplementary Figure S5.2.

A

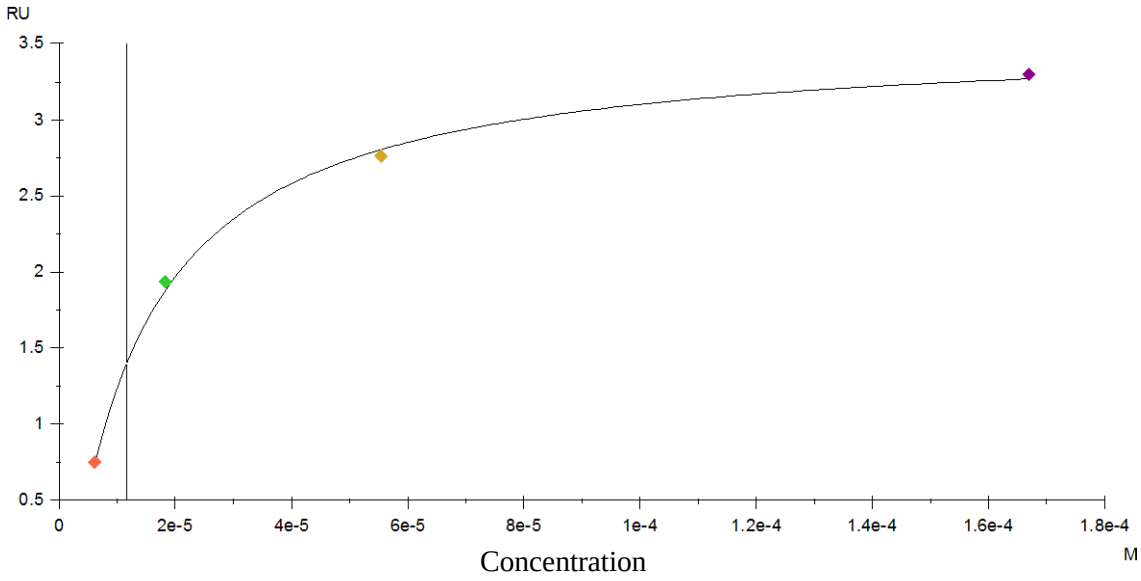

KD (M)	Rmax (RU)	offset (RU)	Chi² (RU²)
1.17E-05	4.281	-0.7322	0.00444

B

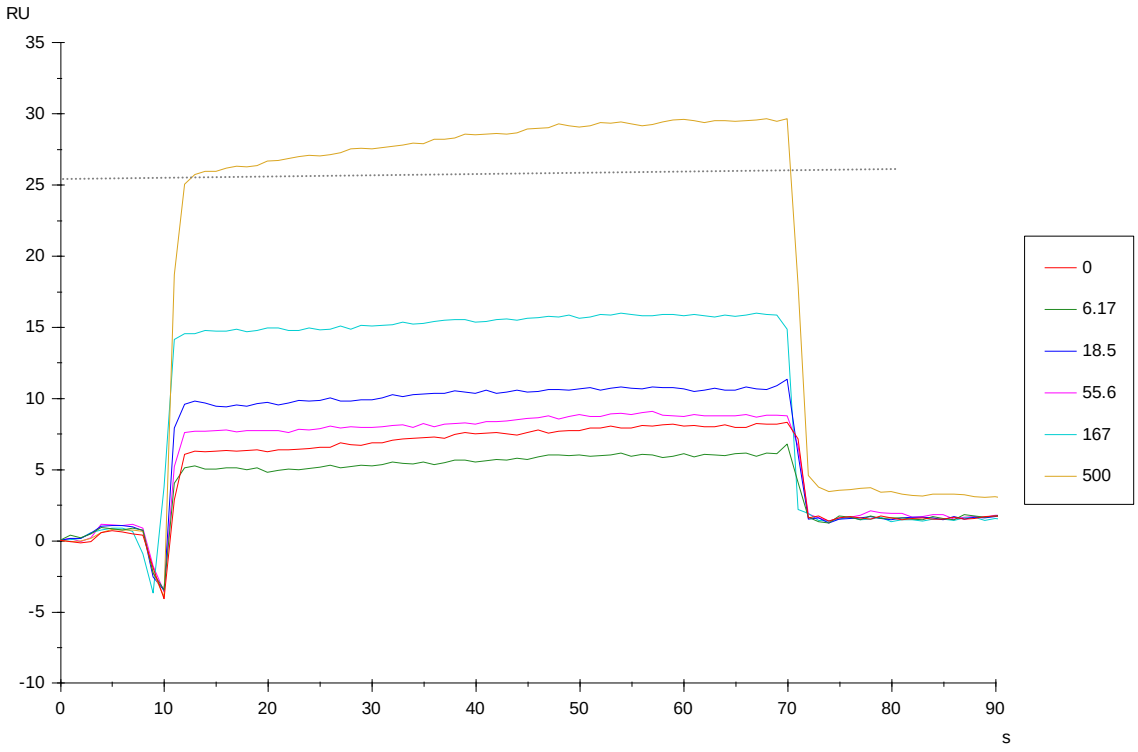

Supplementary Figure S5.4 Biacore steady-state affinity model for the arginine aptamer sequence. (A) The sensorgrams from the arginine binding assays were fit to a steady-state affinity model as described in Supplementary Figure S5.2. (B) The assay performed at 500 μM arginine was excluded from the analysis due to non-specific binding to the reference flow cell. The non-specific binding was observed by the difference between the response curve and the dashed line.

Supplementary Table S5.1 Sequences of aptamers used in this work. The T7 promoter region is indicated in bold and the poly-A linker sequence is indicated in italics.

Aptamer	Sequence
Theophylline	**TTCTAATACGACTCACTATAGGG**AAGTGATACCAGCATCGTCTTGATGCCCTTGGCAGCACTTCCCCC*AAAAAAAAAAAAAAAAAAAAAA*
Citrulline	**TTCTAATACGACTCACTATAGGG**ACGAGAAGGAGTGCTGGTTATACTAGCGGTTAGGTCACTCGTCCCCC*AAAAAAAAAAAAAAAAAAAAAAAA*
Arginine	**TTCTAATACGACTCACTATAGGG**ACGAGAAGGAGCGCTGGTTATACTAGCAGGTAGGTCACTCGTCCCCC*AAAAAAAAAAAAAAAAAAAAAAAA*

Acknowledgements

This work was supported by the National Institutes of Health (R01GM086663), the National Science Foundation (CBET-0917638, CCF-0943269), the Defense Advanced Research Projects Agency (HR0011-11-2-0002), and the Alfred P. Sloan Foundation (fellowship to CDS).

References

1. Hermann, T. and Patel, D.J. (2000) Adaptive recognition by nucleic acid aptamers. *Science*, **287**, 820-825.
2. Ellington, A.D. and Szostak, J.W. (1990) In vitro selection of RNA molecules that bind specific ligands. *Nature*, **346**, 818-822.
3. Tuerk, C. and Gold, L. (1990) Systematic evolution of ligands by exponential enrichment: RNA ligands to bacteriophage T4 DNA polymerase. *Science*, **249**, 505-510.
4. Wieland, M., Benz, A., Klauser, B. and Hartig, J.S. (2009) Artificial ribozyme switches containing natural riboswitch aptamer domains. *Angew Chem Int Ed Engl*, **48**, 2715-2718.
5. Dixon, N., Duncan, J.N., Geerlings, T., Dunstan, M.S., McCarthy, J.E., Leys, D. and Micklefield, J. (2010) Reengineering orthogonally selective riboswitches. *Proc Natl Acad Sci U S A*, **107**, 2830-2835.
6. Greenleaf, W.J., Frieda, K.L., Foster, D.A., Woodside, M.T. and Block, S.M. (2008) Direct observation of hierarchical folding in single riboswitch aptamers. *Science*, **319**, 630-633.
7. Jenison, R.D., Gill, S.C., Pardi, A. and Polisky, B. (1994) High-resolution molecular discrimination by RNA. *Science*, **263**, 1425-1429.
8. Brockstedt, U., Uzarowska, A., Montpetit, A., Pfau, W. and Labuda, D. (2004) In vitro evolution of RNA aptamers recognizing carcinogenic aromatic amines. *Biochem Biophys Res Commun*, **313**, 1004-1008.

9. Famulok, M. (1994) Molecular Recognition of Amino Acids by RNA-Aptamers: An L-Citrulline Binding RNA Motif and Its Evolution into an L-Arginine Binder. *Journal of the American Chemical Society*, **116**, 1698-1706.

10. Mannironi, C., Di Nardo, A., Fruscoloni, P. and Tocchini-Valentini, G.P. (1997) In vitro selection of dopamine RNA ligands. *Biochemistry*, **36**, 9726-9734.

11. Lorsch, J.R. and Szostak, J.W. (1994) In vitro selection of RNA aptamers specific for cyanocobalamin. *Biochemistry*, **33**, 973-982.

12. Muller, M., Weigand, J.E., Weichenrieder, O. and Suess, B. (2006) Thermodynamic characterization of an engineered tetracycline-binding riboswitch. *Nucleic Acids Res*, **34**, 2607-2617.

13. Rich, R.L., Papalia, G.A., Flynn, P.J., Furneisen, J., Quinn, J., Klein, J.S., Katsamba, P.S., Waddell, M.B., Scott, M., Thompson, J. *et al.* (2009) A global benchmark study using affinity-based biosensors. *Anal Biochem*, **386**, 194-216.

14. Leonard, P., Hearty, S. and O'Kennedy, R. (2011) Measuring protein-protein interactions using Biacore. *Methods Mol Biol*, **681**, 403-418.

15. Katsamba, P.S., Park, S. and Laird-Offringa, I.A. (2002) Kinetic studies of RNA-protein interactions using surface plasmon resonance. *Methods*, **26**, 95-104.

16. Win, M.N., Klein, J.S. and Smolke, C.D. (2006) Codeine-binding RNA aptamers and rapid determination of their binding constants using a direct coupling surface plasmon resonance assay. *Nucleic Acids Res*, **34**, 5670-5682.

17. Myszka, D.G. (2004) Analysis of small-molecule interactions using Biacore S51 technology. *Anal Biochem*, **329**, 316-323.

18. Cannon, M.J., Myszka, D.G., Bagnato, J.D., Alpers, D.H., West, F.G. and Grissom, C.B. (2002) Equilibrium and kinetic analyses of the interactions between vitamin B(12) binding proteins and cobalamins by surface plasmon resonance. *Anal Biochem*, **305**, 1-9.

19. Cannon, M.J., Papalia, G.A., Navratilova, I., Fisher, R.J., Roberts, L.R., Worthy, K.M., Stephen, A.G., Marchesini, G.R., Collins, E.J., Casper, D. *et al.* (2004) Comparative analyses of a small molecule/enzyme interaction by multiple users of Biacore technology. *Anal Biochem*, **330**, 98-113.

20. Murphy, M., Jason-Moller, L. and Bruno, J. (2006) Using Biacore to measure the binding kinetics of an antibody-antigen interaction. *Current protocols in protein science*, **Chapter 19**, Unit 19 14.

21. Kwon, M., Chun, S.M., Jeong, S. and Yu, J. (2001) In vitro selection of RNA against kanamycin B. *Molecules and Cells*, **11**, 303-311.

22. Gebhardt, K., Shokraei, A., Babaie, E. and Lindqvist, B.H. (2000) RNA aptamers to S-adenosylhomocysteine: kinetic properties, divalent cation dependency, and comparison with anti-S-adenosylhomocysteine antibody. *Biochemistry*, **39**, 7255-7265.

23. Davis, J.H. and Szostak, J.W. (2002) Isolation of high-affinity GTP aptamers from partially structured RNA libraries. *Proc Natl Acad Sci U S A*, **99**, 11616-11621.

24. de-los-Santos-Alvarez, N., Lobo-Castanon, M.J., Miranda-Ordieres, A.J. and Tunon-Blanco, P. (2009) SPR sensing of small molecules with modified RNA aptamers: detection of neomycin B. *Biosensors & Bioelectronics*, **24**, 2547-2553.

25. Myszka, D.G. (2000) Kinetic, equilibrium, and thermodynamic analysis of macromolecular interactions with BIACORE. *Methods Enzymol*, **323**, 325-340.

26. Jucker, F.M., Phillips, R.M., McCallum, S.A. and Pardi, A. (2003) Role of a heterogeneous free state in the formation of a specific RNA-theophylline complex. *Biochemistry*, **42**, 2560-2567.

27. Zadeh, J.N., Steenberg, C.D., Bois, J.S., Wolfe, B.R., Pierce, M.B., Khan, A.R., Dirks, R.M. and Pierce, N.A. (2011) NUPACK: Analysis and design of nucleic acid systems. *Journal of Computational Chemistry*, **32**, 170-173.

28. Misono, T.S. and Kumar, P.K. (2005) Selection of RNA aptamers against human influenza virus hemagglutinin using surface plasmon resonance. *Anal Biochem*, **342**, 312-317.

29. Liang, J.C., Bloom, R.J. and Smolke, C.D. (2011) Engineering biological systems with synthetic RNA molecules. *Mol Cell*, **43**, 915-926.

30. Myszka, D.G. (1999) Improving biosensor analysis. *J Mol Recognit*, **12**, 279-284.